Superconductivity and Cryogenics
Vol.11, No.2, (2009), pp.20~24

Operating analysis of linear type magnetic flux pump

Y.D. Chung[1,*], S.E. Yang[2] and T.K. Ko[2]

[1]Department of Electrical Engineering, the University of Suwon,
San 2-2 Wau-ri, Bongdam-eup, Hwaseong-si, Gyeonggi-do, 445-743, Korea
[2]Department of Electrical and Electronic Engineering, Yonsei University,
134 Sinchon-dong, Seodaemun-gu, Seoul, 120-749, Korea

Received 30 July 2008; accepted 11 May 2009

***Abstract*-- In order to explain the operating characteristics of LTMFP in a wide range of driving frequency, an analytical equation that takes into account the detailed behavior of the normal spot is necessary. In this paper, based on the phenomenon of magnetic diffusion of the superconductor we modified the theoretical equations for pumping action in LTMFP. The modified equations explained well the pumping actions under the different load magnets. These results are important to explain the pumping tendency of the LTMFP according to driving frequency.**

1. INTRODUCTION

For the applications of superconducting magnet systems, in order to obtain a high magnetic field with stabilized property, the technology of maintenance of the persistent current mode has currently been recognized to be one of the most important problems. In order to achieve to persistent current mode in the hybrid NMR magnet, we designed the linear-type magnetic flux pump (LTMFP) as a current compensator.

The fundamentally operating characteristics of the fabricated LTMFP were investigated: the pumping performance depended on the driving frequency [1-3]. In order to explain the operating characteristics of LTMFP in the wide ranges of load magnet scales, new analytical equations that take into account the detailed behavior of the normal spot are necessary. From this point of view, we present a modification to explain the operating characteristics of LTMFP. The modified equation is induced by the basic mechanism for flux pump and the phenomenon of magnetic diffusion in the superconductor. The key point of the modification is that the size of the normal spot is to be changeable depending on the driving frequency. The change of the normal spot area under the moving flux was already confirmed by magnetic diffusion of superconductor [4].

The main purpose of this study is to explain the performance characteristics of pumping actions according to the driving frequency by use of the modified theoretical mechanism. The pumping tendency according to the driving frequency is calculated under different scales of the load magnet. The measured pumping currents are explained based on the obtained enhancing rates of normal spot, k that is estimated by the modified theoretical equations.

* Corresponding author: ydchung@suwon.ac.kr

2. MODIFIED EQUATIONS FOR PUMPING CURRENT UNDER THE MOVING FLUX

2.1. Structure and Basic Equations of Pumping Current

The LTMFP mainly consists of LTS Nb foil, AC coil, DC bias coil, and laminated iron core as shown in Fig. 1. The traveling magnetic field is realized by means of three phase armature windings. The DC bias current and AC current realize the homopolar traveling magnetic field that is penetrated into the Nb foil of the air gap. The moving speed of the traveling magnetic field is controlled by the driving frequency of AC current. The pumped current I_n surrounding the normal spot is generated by the penetration of traveling magnetic field.

Fig. 2 shows the simplified schematic illustration of the homo-polar traveling magnetic field (its velocity: v) applied to the Nb foil that is connected to the superconducting load magnet. The symbols of z, d, v, W, R_n, w, and h represent the thickness of Nb foil, the gap between slot and Nb foil, the moving velocity of normal spot, the total width of the Nb foil, the resistance of normal spot, the width of normal spot, and the length of normal spot, respectively.

Fig. 3 shows the schematic diagram of (a) invasion of the normal spot in the Nb foil and (b) the corresponding equivalent circuit. In the figure, the normal spot apparently

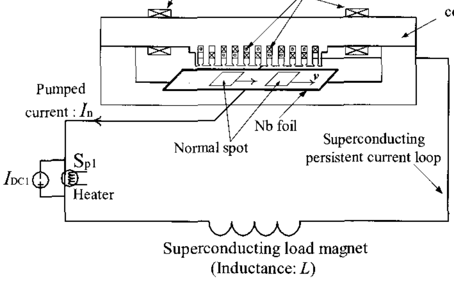

Fig. 1. Connection diagram of the LTMFP system.

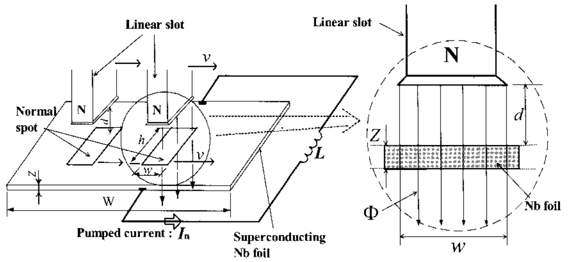

Fig. 2. Schematic diagram of traveling normal spot on the superconducting Nb foil in the LTMFP.

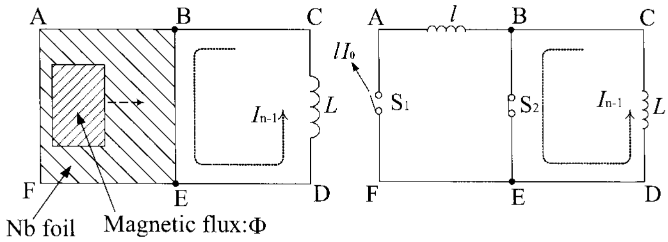

(a) connection diagram (b) equivalent circuit

Fig. 3. Schematic diagram of the invasion of the normal spot.

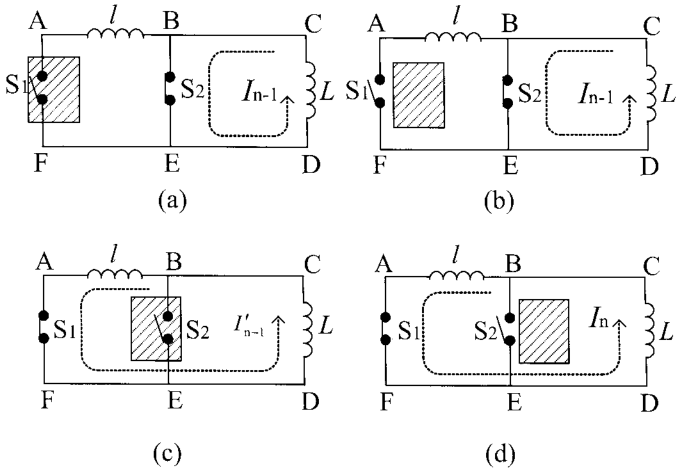

Fig. 4. Basic pumping sequences according to the position of normal spot.

plays an on-off switching element according to its position. The loops ABEF and BCDE, respectively, include an Nb foil and the load magnet. When the normal spot is not yet invaded in the Nb foil, the switches S_1 and S_2 are turned on in the state. However, in the case of S_1 opening (that means the normal spot is inside of the Nb foil), the value of magnetic flux $\Phi_0 = l \cdot I_0$ is released per one cycle as shown in Fig. 3 (b). Thus, the resultant value of the pumped current, $\triangle I_n$, through the persistent current loop is expressed as,

$$\Delta I_n = \frac{\Phi - l \cdot I_0}{L} \tag{1}$$

Fig. 4 illustrates the basic pumping sequences according to the positions of the normal spot. The descriptions of these steps are as follows:

Figure (a): the current I_{n-1} initially flows through the loop BCDE. The magnetic flux Φ begins to enter the Nb foil at this step (S_1:open).

Figure (b): the S_1 is still open due to the time delay for recovery from normal to superconducting transition. The changed value of magnetic flux is $\Phi - l \cdot I_{n-1}$.

Figure (c): Φ begins to leave the Nb foil. The S_1 is now in on state. The induced current I'_{n-1} flows the loop ACDF since S_2 is opened. Here, the current I'_{n-1} is obtained as follows:

$$I'_{n-1} = \frac{L}{L+l} I_{n-1} \tag{2}$$

Figure (d): Φ leaves the Nb foil. The induced I_n flows through the loop ACDF since S_2 is still open due to the time delay for recovery from normal to superconducting transition. The changed amount of magnetic flux, Δ Φ, is expressed as,

$$\Delta\Phi = \Phi - l \cdot I_{n-1} \tag{3}$$

The induced pumped current at the n[th] cycle, I_n, can then be given by

$$I_n = I'_{n-1} + \frac{\Delta\Phi}{L+l} \tag{4}$$

By using the Eqs. (2), (3) and (4), the summed pumping current $I(t)$ according to operating time is expressed as,

$$I(t) = \frac{\Phi}{2l}\left\{1 - \exp\left(-\frac{2l}{T(L+l)} t_n\right)\right\} \tag{5}$$

This is a basic equation of moving normal spot to the position of normal spot [5]. As the LTMFP always produces two normal spots at the Nb foil, referred to the over-mentioned pumping sequence, the equation of pumped current $I(t)$ in LTMFP can be expressed as,

$$I(t) = \frac{\Phi}{2l}\left(1 - \frac{l}{R_n T}\right)\left[1 - \exp\left\{-\frac{4l}{T(L+2l)} t_n\right\}\right] \tag{6}$$

where T means a period for pumping sequence. Since the frequency f is defined as $1/T$, the Eq. (6) is rewritten as,

$$I(t) = \frac{\Phi}{2l}\left(1 - \frac{f\,l}{R_n}\right)\left[1 - \exp\left\{-\frac{4f\,l}{L+2l} t_n\right\}\right] \tag{7}$$

The expressions of l, R_n, and Φ are defined as follows; $l = \mu_0 \times S_n / d$, ($S_n = w \times h$: area of the normal spot, μ_0 (=$4\pi \times 10^{-7}$ H/m): magnetic permeability of the vacuum), $R_n = \rho \times h / z \times w$ (ρ (=1×10^{-8} Ωm): resistivity of the normal spot) [6], and $\Phi = B \times S_n = B \times w \times h$.

2.2. Phenomenon of Enhancement of Normal Spot under the Flux Moving

The above-mentioned Eq. (7) was based on the simple assumption that the size of the normal spot is always constant during operation. However, the analytical equation could not explain the current pumping characteristics under the wide range of driving frequencies. From this reason, we suggest a new analytical condition that takes into account the detailed behavior of the normal spot. This analytical mechanism is based on the phenomenon of the enhancement of the normal spot in the moving penetration flux. This phenomenon explains the enlargement of the region of the normal spot according to the driving frequency. After all, when the width of the normal spot is enhanced according to the driving frequency, the resistance of the normal spot R_n is influenced by the enhanced width w_n. Thus, the influenced parameters are modified as a function of the frequency f.

$$w_n(f) = w_0 + kf = \alpha \quad (8)$$

$$R_n(f) \propto 1/\alpha \quad (9)$$

where the parameter k represents the enhancement rate of the normal spot under the moving flux. The unit is mm/Hz. This conceptual phenomenon is based on the magnetic diffusion of the superconductor.

3. EXPERIMENTAL RESULTS

Fig. 5 provides the illustration of current pumping system under the 6-coil load magnet of 543 mH. In order to reduce the distortion of the output current waveform, a 3-phase reactor is connected at the output of the 3-phase inverter. The cryogenic Hall sensor, which is also installed in the load magnet, measures the pumping current.

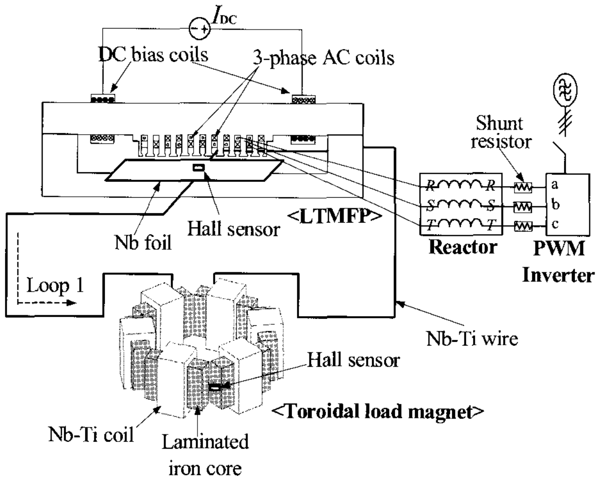

Fig. 5. Connection diagram of current pumping system with different load magnets.

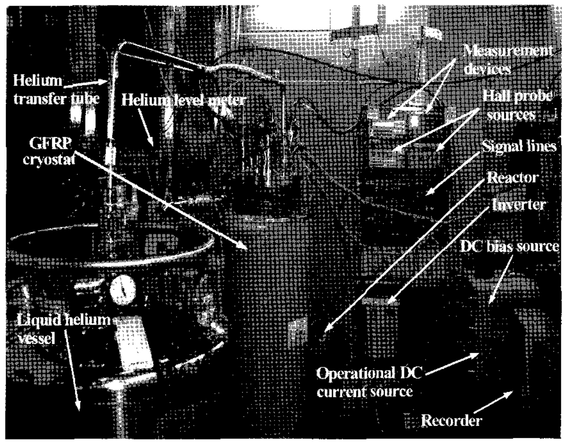

Fig. 6. Photograph of the experimental setup.

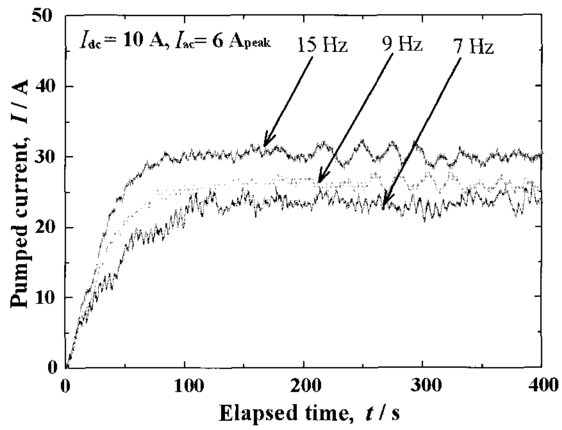

Fig. 7. Measured results of the pumped current with DC bias current at 10 A and AC current at 6 A_{peak} under the load magnet of 1.3 mH. The measured temperature is 4.2 K.

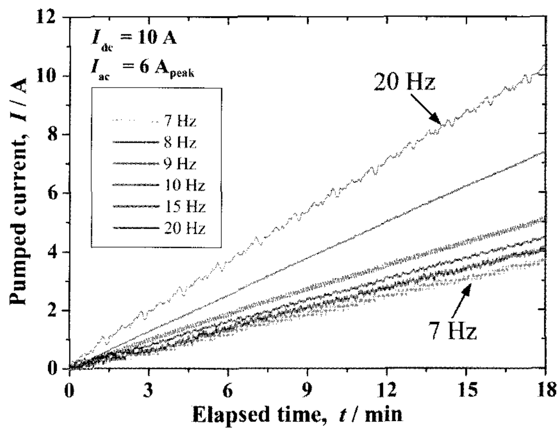

Fig. 8. Measured results of the pumped current with DC bias current at 10 A and AC current at 6 A_{peak} under the load magnet of 543 mH. The measured temperature is 4.2 K.

Fig. 6 shows the photograph of the experimental setup. Both the LTMFP and the superconducting load magnet are installed in the GFRP cryostat. In order to carry out the experiment, liquid helium is transferred into the cryostat from the vessel through the helium transfer tube. A PWM inverter is utilized for the operation of the LTMFP.

Fig. 7 also shows the measured results of the pumped current with DC bias current at 10 A and AC current at 6 A_{peak} under the load magnet of 1.3 mH. Its duration is 400 seconds. Under these driving conditions, the measured results at 7, 9, and 15 Hz become 22.7, 25.3, and 29.8 A, respectively. It has been observed that the pumped current also shows the frequency dependency. As the 3-phase reactor was not installed in the 3-phase inverter, the pumping currents contained some noise and vibration due to the harmonics.

Fig. 8 also shows the measured and calculated results of the pumped current with DC bias current at 10 A and AC current at 6 A_{peak} in the duration of 18 minutes. Under these driving conditions, the measured results at 7, 8, 9, 10, 15, and 20 Hz become 3.6, 4.1, 4.4, 5.0, 7.3, and 10.2 A, respectively. As 3-phase reactors were installed, noise and vibration of pumped currents were remarkably reduced.

4. CALCULATIONS RESULTS FOR CURRENT UNDER DIFFERENT SCALES OF LOAD MAGNET

The measured results of the pumped current are estimated based on the modified analytical equations, i.e., Eqs. (7), (8), and (9).

Fig. 9 shows the calculated results of the pumped current with DC bias current at 10 A and AC current at 6 A_{peak} for different frequencies, i.e., 7, 9, and 15 Hz. The inductance is 1.3 mH. The elapsed time is 400 s. It can be seen that the pumped currents saturate around $t = 100$ s because of the small inductance value of the load magnet. The saturation value of the pumped currents is in proportion to the driving frequency as shown in Fig. 7. It has been observed that pumping current depends on the driving frequency. Based on the experimental results and modified Eqs. (7), (8), and (9), we obtained enhancing rates of normal spot, $k = 0.14$ mm/Hz. The calculated results of pumping current with $k = 0.14$ mm/Hz agreed with the measured results of Fig. (7).

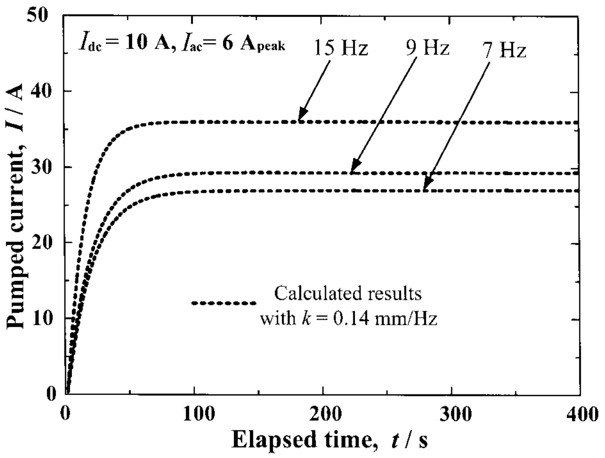

Fig. 9. Calculated results of the pumped current with $k = 0.14$ mm/Hz. The inductance of the load magnet is 1.3 mH.

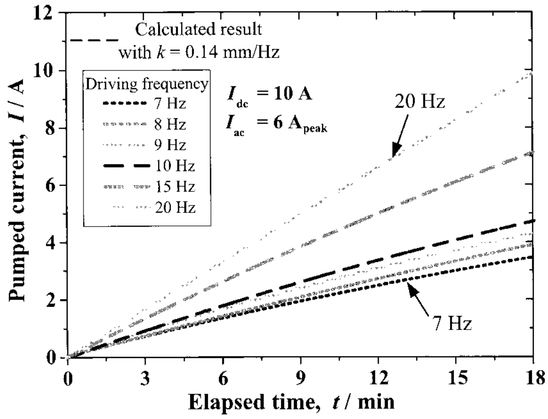

Fig. 10. Calculated results of the pumped current with $k = 0.14$ mm/Hz. The inductance of the load magnet is 543 mH.

In order to verify the estimated value of k, the k value is calculated under the different scale of the load magnet. Fig. 10 also shows the calculated results of the pumped current with DC bias current at 10 A and AC current at 6 A_{peak} in the duration of 18 minutes. The inductance of magnet is 543 mH. Under these driving conditions, the calculated results, which was calculated with $k = 0.14$ mm/Hz, at 7, 8, 9, 10, 15, and 20 Hz become 3.4, 3.9, 4.3, 4.7, 7.0, and 9.9 A, respectively. Thus, it has been investigated the pumping actions of the LTMFP is dominated by the driving frequency. The calculated results for pumping current with $k = 0.14$ mm/Hz have a good agreement with the reported measured results. Thus, that means that the validity of the obtained enhancing rate of the normal spot ($k = 0.14$ mm/Hz) is confirmed under below 20 Hz.

5. CONCLUSIONS

The measured pumping actions according to the driving frequency were explained by the modified theoretical equations. Through the phenomenon of magnetic diffusion under moving flux, enhancing rates of normal spot k, i.e., $k = 0.14$ mm/Hz was estimated. These obtained results have good agreements with measured results under different magnets. Consequently, the modified theoretical mechanism can be considered as a reasonable option to explain the pumping actions under the moving flux for the LTMFP.

REFERENCES

[1] Y.D. Chung, T. Hoshino, T. Nakamura, "Current pumping performance of linear-type magnetic flux pump," *IEEE Trans Appl Superconduct*, vol. 16, no. 2, pp. 1638-1641, 2006.

[2] Y.D. Chung, I. Muta, T. Hoshino, T. Nakamura, "Characteristics of a persistent current compensator for superconducting NMR magnets using linear type magnetic flux pump," *IEEE Trans Appl Superconduct*, vol. 15, no. 2, pp. 1338-1341, 2005.

[3] Y.D. Chung, T. Hoshino, T. Nakamura, "Current pumping performance of linear-type magnetic flux pump with use of feedback control circuit system," *IEEE Trans Appl Superconduct*, vol. 16, no. 2, pp. 1638-1641, 2006.

[4] M.N. Wilson, "Superconducting magnets," Clarendon Press, pp. 143-144, 1983.

[5] Van de Klundert LJM, Ten Kate HHJ, "Fully superconducting rectifiers and fluxpumps," *Cryogenics*, vol. 21, pp. 195-206, 1981.

[6] I. Muta, H. Tsukiji, T. Itoh, S. Ishii, T. Hoshino, E. Mukai, "Superconducting dynamo and its application to superconducting generator," *Cryogenics*, vol. 30, pp. 749-752, 1990.